HHS Public Access

Author manuscript

J Physiol. Author manuscript; available in PMC 2024 April 01.

Published in final edited form as:

J Physiol. 2023 April ; 601(8): 1407–1424. doi:10.1113/JP284026.

Antagonism of TRPV4 channels partially reduces mechanotransduction in rat skeletal muscle afferents

Ayumi Fukazawa[*,1], **Amane Hori**[*,2,3], **Norio Hotta**[2,4], **Kimiaki Katanosaka**[2,4], **Juan A. Estrada**[1], **Rie Ishizawa**[1], **Han-Kyul Kim**[5], **Gary A. Iwamoto**[6], **Scott A. Smith**[1], **Wanpen Vongpatanasin**[5], **Masaki Mizuno**[1]

[1]Department of Applied Clinical Research, University of Texas Southwestern Medical Center, Dallas, TX 75390, USA

[2]Graduate School of Life and Health Sciences, Chubu University, Kasugai 487-850, Japan

[3]Japan Society for the Promotion of Science, Tokyo 102-8472, Japan

[4]College of Life and Health Sciences, Chubu University, Kasugai 487-850, Japan

[5]Department of Internal Medicine, University of Texas Southwestern Medical Center, Dallas, TX 75390, USA

[6]Department of Surgery, University of Texas Southwestern Medical Center, Dallas, TX 75390, USA

Abstract

Mechanical distortion of working skeletal muscle induces sympathoexcitation via thin fibre afferents, a reflex response known as the skeletal muscle mechanoreflex. However, to date, the receptor ion channels responsible for mechanotransduction in skeletal muscle remain largely undetermined. Transient receptor potential vanilloid 4 (TRPV4) is known to sense mechanical stimuli such as shear stress or osmotic pressure in various organs. It is hypothesized that TRPV4 in thin-fibre primary afferents innervating skeletal muscle is involved in mechanotransduction. Fluorescence immunostaining revealed that 20.1 ± 10.1% of TRPV4 positive neurons were expressed with DiI-labeled small dorsal root ganglia (DRG) neurons, and 9.5 ± 6.1% of TRPV4 were co-localized with C-fibre marker, peripherin-positive neurons. *In vitro* whole-cell patch clamp recordings from cultured rat DRG neurons demonstrated that mechanically-activated current amplitude was significantly attenuated after the application of the TRPV4 antagonist, HC067047 compared to control ($P = 0.004$). Such reductions were also observed in single-fibre recordings from a muscle-nerve *ex vivo* preparation where HC067047 significantly decreased

Correspondence: Masaki Mizuno, Ph.D., Department of Applied Clinical Research, School of Health Professions, University of Texas Southwestern Medical Center, 5323 Harry Hines Boulevard, Dallas, Texas 75390-9174, USA, Tel: +1-214-648-9188, FAX: +1-214-648-3566, masaki.mizuno@utsouthwestern.edu.

*Contributed equally to this study

AUTHORS CONTRIBUTIONS

MM conceived and designed experiments. AF, AH, and JAE performed experiments. AF, AH, NH, and MM analyzed data. AF, AH, NH, KK, JAE, RI, HKK, GAI, WV, SAS, and MM interpreted results of experiments. AF, AH, NH, and MM prepared figures. AF and MM drafted the manuscript or revised it critically for important intellectual content. AF, AH, NH, KK, JAE, RI, HKK, GAI, WV, SAS, and MM have read and approved the final version of this manuscript.

COMPETING INTERESTS

The authors declare that they have no competing interests.

afferent discharge to mechanical stimulation ($P = 0.007$). Likewise, in an *in vivo* decerebrate rat preparation, the renal sympathetic nerve activity (RSNA) and mean arterial pressure (MAP) responses to passive stretch of hindlimb muscle were significantly reduced by intraarterial injection of HC067047 (ΔRSNA: $P = 0.019$, ΔMAP: $P = 0.002$). The findings suggest that TRPV4 plays an important role in mechanotransduction contributing to the cardiovascular responses evoked by the skeletal muscle mechanoreflex during exercise.

Graphical Abstract

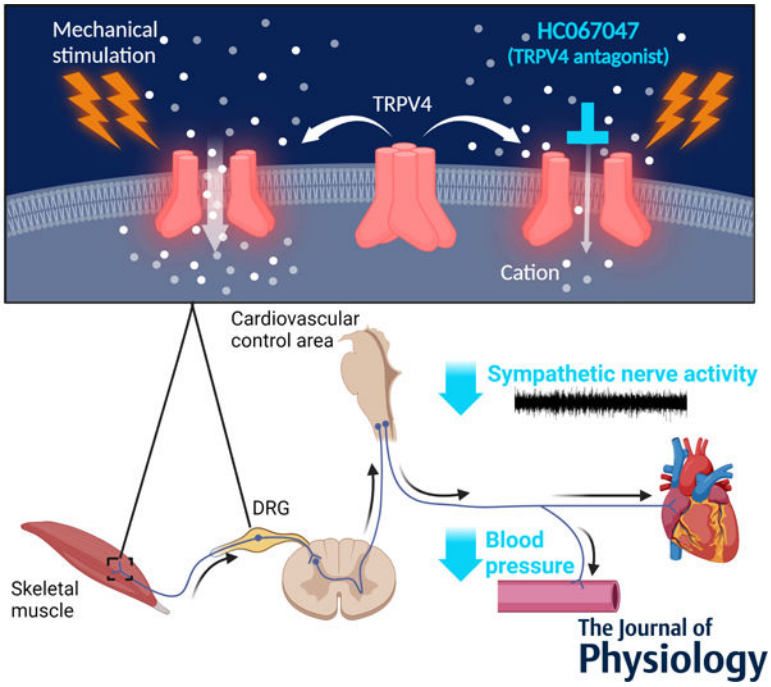

Blocking transient receptor potential vanilloid 4 (TRPV4) channels has an inhibitory effect on sympathetic and pressor responses to mechanical stimulation by attenuating mechanotransduction in sensory afferents innervating skeletal muscle. The TRPV4 antagonist, HC067047, reduces the responsiveness of thin fibre muscle afferents and small dorsal root ganglion neurons to mechanical stimulation. Furthermore, it is demonstrated that intraarterial injection of HC067047 suppresses the sympathetic nerve activity and blood pressure responses to passive hindlimb muscle stretch in vivo. These findings suggest that TRPV4 may play a crucial role in mechanotransduction contributing to the cardiovascular responses evoked by the skeletal muscle mechanoreflex during exercise. Design made in BioRender.

Keywords

transient receptor potential vanilloid 4; mechanotransduction; muscle mechanoreflex; group IV muscle afferents; primary sensory neuron

Introduction

The sympathetic nervous system plays a crucial role in the regulation of the cardiovascular system during exercise. Adjustments in sympathetic outflow mediating the cardiovascular response to physical activity are, in part, mediated by mechanically sensitive skeletal muscle afferents stimulated by mechanical distortion of working skeletal muscle (Kaufman *et al.*, 1984; Stebbins *et al.*, 1988; Victor *et al.*, 1989; Williamson *et al.*, 1994; Hayes *et al.*, 2005). However, to date, the receptor mechanisms responsible for skeletal muscle mechanotransduction have not been fully identified (Smith *et al.*, 2014).

Transient receptor potential vanilloid 4 (TRPV4), a multimodally activated, nonselective cation channel, has been detected in endothelial cells (Watanabe *et al.*, 2002a; Watanabe *et al.*, 2002b), smooth muscle cells (Filosa *et al.*, 2013) and dorsal root ganglion (DRG) neurons (Grant *et al.*, 2007; Zhang *et al.*, 2008). TRPV4 was first identified as an osmosensitive channel due to its activation by hypotonicity (Liedtke *et al.*, 2000; Strotmann *et al.*, 2000). It can likewise be activated by mechanical forces such as shear stress (Swain & Liddle, 2021), stretch (Loukin *et al.*, 2010) and surface expansion (Michalick & Kuebler, 2020). In addition, recent evidence suggests that TRPV4 is involved in the response to noxious mechanical stimulation of the normal joint in rats (Richter *et al.*, 2019). The precise mechanisms underlying mechanical force-induced TRPV4 activation are currently not completely understood. Although direct (deformation of plasma membrane) or indirect (intracellular signaling cascades) mechanical activation of TRPV4 have been proposed (Kung, 2005; Christensen & Corey, 2007; Michalick & Kuebler, 2020), the role TRPV4 plays in activation of skeletal muscle afferent fibres and muscle mechanotransduction have not been determined.

We therefore hypothesized that the muscle mechanoreflex is, in part, mediated by activation of TRPV4 in skeletal muscle afferents. To test this hypothesis, we examined whether application of a TRPV4 antagonist attenuates 1) whole-cell current responses to mechanical stimuli in small DRG neurons, 2) responsiveness to mechanical stimuli in thin-fibre muscle afferents and 3) muscle mechanoreflex responses to passive stretch in healthy rats. We further investigated whether TRPV4 and the afferent marker peripherin are co-localized in DRG neurons subserving thin-fibre skeletal muscle afferents using a retrograde tracing technique.

Methods

Ethical approval

All studies were performed in accordance with the US Department of Health and Human Services NIH *Guide for the Care and Use of Laboratory Animals*. All experimental procedures were approved by the Institutional Animal Care and Use Committee of the University of Texas Southwestern Medical Center (no.2019-102849) and the Animal Care Committee of Chubu University (no. 202010005, revision no. 22–053). All authors understood and conformed to the guidelines and ethical principles of *The Journal of Physiology* (Grundy, 2015).

Animals

Forty-four male Sprague-Dawley rats (10–19 weeks, body weight (BW): 401.3 ± 67.7 g) (Envigo, Indianapolis, IN, USA or SLC, Shizuoka, Japan) were used for immunohistochemistry, whole-cell patch clamp recording and single fibre recording. Animals had free access to food and water. The animals were kept one to four per cage under 12 h light/dark cycle in an air-conditioned room (22–24˚C) until required for experiments.

Labeling DRG neurons innervating hindlimb skeletal muscle

We modified methods that have been used previously (Xing & Li, 2017; Schiller *et al.*, 2019). Three rats (11 weeks and BW: 318.0 ± 8.7 g) were anaesthetized by inhalation of an isoflurane-oxygen mixture (2–4% isoflurane in 100% oxygen). Depth of anesthesia was assessed and monitored via tail pinch throughout the procedure. The adequacy of anesthesia was verified by lack of a withdrawal response to tail pinch. The skin was incised and pulled away from underlying muscle tissue. Subsequently, the fluorescent retrograde tracer 1,1-dioctadecyl-3,3,3,3-tetramethylindocarbocyanine perchlorate (DiI, 60 mg/mL, Sigma, St Louis, MO, USA) was injected into the white portion of the gastrocnemius muscle (Ariano *et al.*, 1973) in order to label muscle afferent DRG neurons. A total of 3 μL DiI was injected, and the needle was left in the muscle for 5 min to prevent leakage of tracer. The skin was then sutured. Following cessation of anesthesia, a single dose of buprenorphine SR (0.06 mg/100 mg body weight) was given. Rats were returned to their cages for 5 days to recover from the procedure and permit the retrograde tracer to be transported to DRG neurons.

Fluorescence immunostaining & triple labelling

Rats were anaesthetized by intraperitoneal injection of euthasol (390 mg/mL pentobarbital sodium and 50 mg/mL phenytoin sodium, 0.1 mL/100 g body weight (0.30–0.35 mL)). The adequacy of anesthesia was verified by lack of a withdrawal response to tail pinch. Rats were then transcardially perfused with saline followed by 4% paraformaldehyde for tissue fixation. The L4–6 DRGs were harvested and post-fixed overnight in 4% paraformaldehyde. The DRGs were dehydrated sequentially in 10% and 20% sucrose, and afterwards sectioned at 10 μm using a cryostat. Co-immunostaining for TRPV4 and peripherin was performed by incubation with rabbit anti-TRPV4 (1:250, cat. no. ACC-034, RRID# AB_2040264, Novus Biological, Littleton, CO, USA) and mouse anti-peripherin (1: 250, cat. no. ab254137, RRID# AB_306848, Abcam, Cambridge, MA, USA) overnight at room temperature (RT), after blocking with 10% normal goat serum/phosphate-buffered saline (PBS) plus either 0.05% Tween 20 or 0.5% Triton X-100 for 1 h. The sections were rinsed in PBS and subsequently incubated with fluorescence-conjugated secondary antibodies (Alexa Fluor 405-conjugated goat anti-rabbit IgG (1:200, cat. no. ab175652, RRID#AB_2687498, Abcam) and Alexa Fluor 488-conjugated goat anti-mouse IgG (1:500, cat. no. A32723, RRID# AB_2633275, Thermo Fisher Scientific, Waltham, MA, USA)) for 1 h at RT.

For quantitative analysis, six or seven sections from each animal were arbitrarily selected (a total of 20 sections). The fluorescence images were observed and captured with a fluorescence microscope system (Axio Imager A2, Zeiss, Oberkochen, Germany). The

number of positively stained small-diameter DRGs neurons (i.e. less than 30 μm in diameter) (Zhang *et al.*, 2014) were counted and the percentage of peripherin- or DiI-positive neurons in TRPV4-positive neurons was calculated.

Whole-cell patch clamp preparation

DRG culture—DRG neurons were prepared as previously reported (Hotta *et al.*, 2019a; Hori *et al.*, 2022). Rats were euthanized by bilateral thoracotomy and removal of the heart under deep isoflurane sedation (4–5% in 100% oxygen). The adequacy of anesthesia was verified by lack of a withdrawal response to tail pinch. Collected DRGs from rats were digested with collagenase IV (1.0 mg/mL, Sigma) for 30 min and trypsin-EDTA (0.05%, Sigma) for 5 min each at 37˚C. Following, the enzyme reaction was terminated by using trypsin inhibitor (0.08 mg/mL, Thermo Fisher Scientific) at RT. DRGs were then washed with Dulbecco's modified Eagle's medium (DMEM)/Ham's F-12 (Thermo Fisher Scientific) supplemented with nerve growth factor (0.1 μg/mL, NGF-7S, Sigma), fetal bovine serum (5%, Sigma), Glutamax (1%, Thermo Fisher Scientific), glucose (0.8%, Sigma), penicillin-streptomycin (10 μL/mL, Sigma), and Dulbecco's phosphate buffered saline (Sigma). DRGs were placed on glass coverslips coated with poly-L-lysine (0.1 mg/mL, Sigma) and laminin (0.13%, Thermo Fisher Scientific) after being suspended and dissociated in the supplemented DMEM/Ham's F-12 solution using a fire-polished Pasteur pipette. DRGs were maintained at 37˚C in a CO_2 incubator replacing with fresh supplemented medium at least every 2 days up to the day of current recording.

Whole-cell patch clamp recording—We recorded inward current and membrane voltages from cultured small DRG neurons (i.e. less than 30 μm in diameter) at RT as described previously (Hotta *et al.*, 2019a; Hori *et al.*, 2022). The patch pipettes were pulled from borosilicate glass capillaries (Narishige, Tokyo, Japan) and filled with a solution containing (mM): 10 NaCl, 130 KCl, 1 EGTA, 1 $MgCl_2$, 10 HEPES, 2 ATP and 0.2 GTP, adjusted to about pH 7.3 with 1M KOH. HEPES-buffered solution containing (mM): 140 NaCl, 5 KCl, 2 $CaCl_2$, 2 $MgCl_2$, 10 glucose and 10 HEPES, adjusted to approximately pH 7.4 with 1M NaOH was used as the extracellular bath solution (2 mL).

Currents and membrane voltages were recorded using Axopatch 200B (Molecular Devices, San Jose, CA, USA). Data were digitized and analyzed using Digidata 1550B (Molecular Devices) and Clampex software (Molecular Devices).

Mechanical stimulation—Mechanically-activated (MA) inward currents were recorded as described previously (Hotta *et al.*, 2019a). MA currents were recorded in the voltage clamp mode at a holding potential of −60 mV. Mechanical stimuli were applied to the cell surface using a heat-polished glass pipette (φ = ~5 μm) as a mechanical probe, which was positioned at an angle of ~45˚ to the cell surface and driven by a piezo-controlled micromanipulator (Nanomotor MM3A; Kleindiek Nanotechnik, Kusterdingen, Germany). From the starting position where the mechanical probe gently touched the cell surface, the probe moved forward to press the cell surface and was kept at this position for 0.5 s, then moved backward to the starting position in each stimulation. The velocity of the movement was 1.8 μm ms^{-1}. A series of mechanical stimuli were applied, in which the

intensity (distance of the probe movement) was increased from 1 to 6–11 steps (a step size was 1 μm/step; i.e. step number = the distance probe moved in μm), with 10 s intervals. The mechanical threshold was defined as the lowest intensity that evoked MA current whose amplitude exceeded 50 pA. This threshold value (50 pA) was based on a previous definition (Xing *et al.*, 2015).

Procedures—The present study consisted of two application trials: control and TRPV4 antagonist trials. One trial was applied to each cell and MA currents were recorded before and after the application. In each trial, first, MA current was recorded to a stepwise-increasing mechanical stimuli up to 6–11 steps as mentioned previously. Then the following test solutions were carefully and locally applied into the extracellular bath solution (i.e. 2 mL of HEPES-buffered solution) using a valve control system (VC-6, Warner Instruments, Holliston, MA, USA). HEPES-buffered solution was used as vehicle in the control trial and 1 μM HC067047 (Sigma) solution was used in the TRPV4 antagonist trial. The concentration was based on a previous study (Harraz *et al.*, 2018). HC067047 (1 mg) was dissolved by 2.12 mL of 70% DMSO: 30% ethanol solution to 1 mM. Then, 1 mM HC067047 stock solution was diluted with vehicle solution (HEPES-buffered solution for *in vitro* studies (10 μL stock solution in 9990 μL HEPES-buffered solution), Krebs-Henselet (Krebs buffer) solution for *ex vivo* studies (1 μL stock solution in 999 μL Krebs buffer solution), and saline for *in vivo* studies (10 μL stock solution in 9990 μL saline)) to 1 μM. The final concentrations of DMSO and ethanol were 0.07% and 0.03%, respectively. Five minutes after the application of the test solution, MA current was again recorded to the same series of mechanical stimuli at the original position.

Analysis—In the present study, we compared not only the mechanical threshold, but also the amplitude of the test substances at the same step number corresponding to the intensity that mechanical threshold was marked before the application. Eight data sets were excluded from analysis for *mechanical threshold* because the amplitude of MA currents did not exceed 50 pA at the maximal intensity and mechanical threshold was not observed after HC067047 application. However, these data sets were included to analyze the *amplitude* of MA current because we succeeded in recording changes at the intensity corresponding to mechanical threshold before the application of test solutions.

The population of increased and decreased mechanical threshold after application of test solutions was calculated. The proportion of DRG neurons classified as having a difference in mechanical threshold (ΔMt) before and after the test applications was based on the threshold before the application. The judgment of the direction of the threshold change was determined as follows: “decreased” after the test application, if ΔMt was more than −2 steps of the mechanical intensity of the threshold before application; “unchanged”, $\Delta Mt \leq \pm 1$ step; “increased”, $\Delta Mt \geq 2$ steps.

Based on time constraint (τ) of MA current inactivation, MA currents have been grouped into three types: rapidly adapting (RA); inter-mediately adapting (IA); and slowly adapting (SA) (Drew *et al.*, 2002; Hu & Lewin, 2006). We calculated τ of current inactivity using a single exponential fitting procedure, via Clampfit software (Molecular Devices), and defined

the currents as RA, $\tau < 3$ ms; IA, $3 \leq \tau \leq 30$ ms; and SA, $\tau > 30$ ms, according to previous studies (Kubo *et al.*, 2012; Hotta *et al.*, 2019a).

Muscle-nerve preparation

Action potential recording—These recordings were made using methodology reported previously (Hotta *et al.*, 2019a; Hori *et al.*, 2022). Extensor digitorum longus muscle (EDL) was excised from rats euthanized with CO_2 along with the common peroneal nerve. The rat was placed in an euthanasia chamber (18L), then 99.9% CO_2 (6–9 L/min) was introduced for 2 to 3 min until lack of respiration and faded eye color were observed. CO_2 flow was maintained for a minimum of 1 min after respiration ceased. Isolated EDL muscle with the common peroneal nerve was placed in a test chamber containing warmed modified Krebs buffer solution (at ~34 ˚C and pH 7.4), which contained (in mM): 1.2 KH_2PO_4, 1.2 $MgSO_4$, 2.5 $CaCl_2$, 4.7 KCl, 20.0 glucose, 25.0 $NaHCO_3$ and 110.9 NaCl, and bubbled with 5% CO_2 + 95% O_2 gas mixture. The common peroneal nerve was drawn into the recording camber filled with paraffin oil. We repeatedly dissected using two sharpened watchmaker forceps and put one placed on a 0.1 mm diameter gold recording electrode until a single group IV fibre was identified.

Subsequently, fibre action potentials were amplified, filtered, and recorded continuously on a computer via PowerLab 16/35 (ADInstruments, Sydney, NSW, Australia). Data was analyzed using Spike Histogram software (ADInstruments).

We used fibre recordings in this experiment if the following three criteria were fulfilled (Taguchi *et al.*, 2005): (1) the fibre responded to gentle probing by a smoothly rounded glass rod to the surface of the EDL, (2) the decrease in discharge rate in response to passive muscle stretching was intensity independent (intensity-dependent discharge is a property typically observed in group I and II muscle spindle afferents that were not the focus of study), and (3) the conduction velocity of the fibre recorded was less than 2.0 m/s (characteristic of group IV fibres) (Lawson & Waddell, 1991). Conduction velocity was calculated from the distance and conduction latency between the stimulation electrodes on the receptive fields and the recording electrode.

Mechanical stimulation—A mechanical stimulus was applied using a mechanical stimulator with feedback regulation force. Once a single group IV afferent fibre was identified, ramped mechanical stimuli, linearly increasing from 0 to 392 mN in 40 s, was applied to the most sensitive point of the identified receptive field using a servo-controlled mechanical stimulator equipped with a 2.3 mm^2 round-tipped probe (Hotta *et al.*, 2019a; Wakatsuki *et al.*, 2021).

Procedures—Similar to DRG experiments, we recorded action potentials of each muscle nerve preparation in 2 different trials: before and after intramuscular administration of vehicle (control trial) and HC067047 (TRPV4 antagonist trial). We applied one trial to each preparation and recorded nerve activities before and after the application. In an administration trial, first, we recorded action potentials elicited by the mechanical stimulus. Then, a 5 μL test solution was injected near the receptive field using a microsyringe with a 30 gauge needle (the injection angle and depth were ~60° to the surface and 1 mm,

respectively). The following test solutions were injected: Krebs buffer solution as a vehicle control (control trial) or 1 μM HC067047 solution (TRPV4 antagonist trial). Five minutes after the injection, the same mechanical stimulus was applied to the original location.

Analysis—The mechanical threshold was identified as the intensity that induced a discharge exceeding the mean frequency + 2 SD of the spontaneous discharge observed during the baseline period, when there were two or more consecutive discharges exceeding this level (Taguchi *et al.*, 2005).

Recording renal sympathetic activity and blood pressure in vivo

General surgical procedures—Rats were anesthetized with 1–4% isoflurane in oxygen and intubated for mechanical ventilation, as described previously (Mizuno *et al.*, 2016; Hori *et al.*, 2022). Depth of anesthesia was assessed and monitored via tail pinch up until the time precollicular decerebration was performed. To stabilize fluid balance and maintain baseline arterial blood pressure (ABP), a sodium bicarbonate solution (8 mL, 1 M $NaHCO_3$ and 40 mL 5% dextrose in 152 mL Ringer solution) was continuously infused into the jugular vein at a rate of 3–5 mL/h/kg. ABP was continuously measured by a pressure transductor (MLT0380/D, ADInstruments) connected to an arterial catheter placed in the left common carotid artery. Electrocardiograph (ECG) recordings were obtained using needle electrodes. A branch of the left renal nerve was attached to bipolar electrodes (OT220-064a, Unique Medical, Osaka, Japan) for renal sympathetic nerve activity (RSNA) recording. The nerve and electrodes were covered with silicone glue (Kwik-Sil, World Precision Instruments, Sarasota, FL, USA) for insulation and fixation. To administer test solutions, the left common iliac artery was catheterized and the tip of the catheter was placed at the bifurcation of the abdominal aorta. To trap injected test solution in the hindlimb and avoid test solution spillover into the systemic circulation, a reversible vascular occluder (18080–01, FST, Foster City, CA, USA) was placed around the abdominal aorta and inferior vena cava just above the aortic bifurcation. Animals were held in stereotaxic head unit (David Kopf Instruments, Tujunga, CA, USA) and then, precollicular decerebration was performed. To minimize cerebral hemorrhage, the remaining intact common carotid artery was isolated and ligated. A bilateral craniotomy was performed by drilling burr holes into the parietal skull. Subsequently, the portion of bone superior to the central sagittal sinus was removed. The dura mater was breached and reflected. The cerebral cortex was gently aspirated to visualize the superior and inferior colliculi. Using a blunt instrument, the brain was sectioned pre-collicularly and the transected forebrain aspirated. Small pieces of oxidized regenerated cellulose were placed on the exposed surfaces of the brain and cotton balls were used to pack the cranial cavity. As precollicular decerebrated rats are insentient and without conscious pain sensation (Silverman *et al.*, 2005), we did not assess withdrawal or blood pressure responses to tail pinch after decerebration. Post-decerebration, isoflurane anesthesia was discontinued and a minimum recovery period of 1 h was employed before beginning any experimental procedure.

Experimental procedures—Mechanically sensitive afferents were preferentially activated via passive hindlimb muscle stretch. To begin, baseline resting tension was set to 70–100 g, and the muscle was contracted by electrical stimulation of the tibial nerve (0.1

ms, 40 Hz, ≤3 × motor threshold) for 30 s. After a >10-min recovery period, the hindlimb muscles were passively stretched at tensions approximately equivalent to those achieved during electrically-induce muscle contraction. To evoke a mechanical stimulus similar to that elicited during muscle contraction, care was taken to generate the same pattern of muscle tension developed during maximal static contractions. This procedure was performed before and after the administration of the test solutions (saline as a vehicle control or 1 μM HC067047 solution as a TRPV4 antagonist trial). 0.1 mL of the test solutions were administered into the arterial supply to the right leg, while the circulation of hindlimb was occluded by the occluder which was released 5 min after administration of the test solutions. Five minutes after the release, isolated stimulation of mechanically sensitive afferent fibres was achieved by passively stretching the triceps surae of the right hindlimb for 30 s. It has been reported that a 0.5% DMSO solution attenuates cardiovascular responses to activation of the exercise pressor reflex (Ducrocq *et al.*, 2019). In a set of corollary experiments, we tested whether the control solution containing 0.07% DMSO and 0.03% ethanol alters the pressor and/or sympathetic responses to passive stretch as compared to saline administration.

End experiment procedures—To validate the RSNA signals recorded from postganglionic renal sympathetic fibres, an intravenous infusion of hexamethonium bromide (60 mg/kg) was given to abolish RSNA at the end of experiments. RSNA background noise was measured over a 30 min period after the insentient decerebrated animal was humanely killed by intravenous injection of saturated potassium chloride (4M, 2 mL/kg).

Analysis—Data were analyzed as previously described (Mizuno *et al.*, 2016). RSNA, ABP, and ECG signals were amplified, filtered and continuously recorded on a computer via PowerLab 16/35 (ADInstruments). We analyzed data using LabChart 8 application software (ADInstruments). To analyze RSNA, full-wave rectified signals of RSNA were used. Mean arterial pressure (MAP) and heart rate (HR) were calculated from ABP and ECG recordings, respectively. Data sets of one-second averages for RSNA, MAP, and HR were analyzed. RSNA, MAP and HR recorded for 30 s immediately before the onset of stretch were used to determine baseline values. Baseline RSNA was designated as 100% and used to quantify RSNA responses to mechanical stimulation. Changes in RSNA (ΔRSNA, %) from baseline were evaluated. The peak response of each variable was defined as the greatest change from baseline elicited by muscle stretch.

Statistical analysis—Statistical analyses were performed using repeated two-way analysis of variance (ANOVA) to examine the effects of test solution (control or HC067047) and trial (before or after application of test solutions). If significant interactions or main effects of test solutions or trials were observed, the Bonferroni's multiple comparison test was performed to examine the differences among groups. Group comparisons (control vs. HC067047) were made via Student unpaired t-test. To compare the ratio of the three types of MA currents and changes of mechanical threshold we recorded between the two trials, we used a Fischer's exact test. Changes of MA current to increasing mechanical stimulus were analyzed with generalized estimating equations.

Analyses were conducted using statistical software (Prism 9.0, GraphPad Software, San Diego, CA, USA, SPSS Statistics 28, IBM Corp., Armonk, NY, USA). Statistical significance was defined as $P < 0.05$. Data are presented as the mean ± SD.

Results

Co-localization of TRPV4 and peripherin in L4-L6 DRG neurons innervating hindlimb muscle

We randomly collected a total of 20 DRG sections from three rats. Sample photos in Figure 1 show that 20.1 ± 10.1% of TRPV4-positive small DRG neurons expressed DiI. Of these, 9.5 ± 6.1% and 10.6 ± 7.2% were peripherin-positive and -negative neurons, respectively.

Whole-cell patch clamp recording of DRG neurons

General results—DRGs were collected from 10 rats and we assessed 42 small DRG neurons that responded to the mechanical stimuli (φ = 26.0 ± 2.2 μm, range: 20.3–29.9 μm). The pipet resistance was 7.8 ± 1.2 MΩ, and the membrane potential was −49.6 ± 7.3 mV before mechanical stimulation. There are 14 MA currents classified as RA (33.3%), 20 as IA (47.6%), and 8 as SA (19.0%). The proportion of MA current types were not significantly different between two trials ($P = 0.356$, Fischer's exact test).

Response to mechanical stimulation—MA currents increased depending on the intensity of mechanical stimuli ($P < 0.0001$, generalized estimating equations). Mean mechanical threshold was 4.2 ± 2.1 steps (n = 42) (step number corresponded to the distance that the mechanical probe moved forward to push the cell surface, i.e. μm) and the amplitude of MA current at the intensity corresponding to mechanical threshold was –92.2 ± 28.4 pA (n = 42).

Figure 2 shows sample recordings of MA currents before and 5 min after the application of either the control or TRPV4 antagonist HC067047 solutions. A significant interaction between trials (before vs. after) and test solutions (control vs. HC067047) was observed ($P = 0.0294$, generalized estimating equations). Moreover, a significant interaction between test solution and trials for MA current amplitude was observed ($P = 0.008$, Fig.3A). Subsequent post hoc tests revealed that the MA current amplitude was significantly decreased 5 min after the application of HC067047 ($P = 0.010$, Bonferroni's multiple comparison test), and that value was significantly lower than 5 min after the application of the control solution ($P = 0.004$, Bonferroni's multiple comparison test, Fig.3A&B).

A significant main effect of test solution on mechanical threshold was observed ($P = 0.004$, Fig.3C).

Figure 3D shows the proportion of increased and decreased mechanical threshold after application of test solutions. There was a significant difference between control and TRPV4 antagonist trials ($P = 0.006$, Fischer's exact test). The application of HC067047 increased mechanical threshold in 66.7% of RA (6 out of 9), 57.1% of IA (4 out of 7) and 100.0% of SA (5 out of 5) neurons while mechanical thresholds in control trials were increased 0.0% of RA (0 out of 5), 30.8% of IA (4 out of 13) and 33.3% of SA neurons (1 out of 3).

Muscle-nerve preparation

General results—We identified 14 mechanosensitive group IV fibres from EDL muscle of 12 rats. The conduction velocity in the group IV afferent fibres was 0.61 ± 0.32 ms^{-1} (range: 0.30–1.45 ms^{-1}).

Response to mechanical stimulation—Figure 4 demonstrates sample recordings of single group IV fibre activity. Action potential discharges were evoked by the ascending ramped pressure to the receptive field of the muscle (0–392 mN in 40 s). Discharge frequency in all single units were increased by the mechanical stimuli (response magnitude = 70.9 ± 47.6 spikes, n = 14). The mean mechanical threshold was 86.4 ± 64.5 mN (n = 14).

Significant interactions between test solution and trial for both mechanical threshold and response magnitude were observed (mechanical threshold: $P = 0.027$, response magnitude: $P = 0.006$, n = 14, Fig.5A&B).

Recording renal sympathetic activity, heart rate and blood pressure in vivo

General results—Figure 6 shows representative recordings of ABP and RSNA responses to passive stretch before and after intraarterial injection of vehicle or HC067047 solutions. We succeeded in measuring ABP in 16, HR in 16 and RSNA in 11 rats.

Baseline MAP, HR and RSNA were not significantly different between control and TRPV4 antagonist groups (baseline MAP: 96 ± 25 mmHg in control trial (n = 7) vs. 110 ± 17 mmHg in HC067047 trial (n = 9), $P = 0.179$, Student unpaired *t*-test; HR: 422 ± 33 beats/min in control trial (n = 7) vs. 423 ± 40 beats/min in HC067047 trial (n = 9), $P = 0.941$, Student unpaired *t*-test; signal to noise ratio of RSNA: 4.75 ± 1.83 in control trial (n = 5) vs. 5.85 ± 1.94 in HC067047 trial (n = 6), $P = 0.360$, Student unpaired *t*-test).

Response to passive stretch—The interaction between test solution and trial for ΔMAP and ΔRSNA was significant (ΔMAP:$P = 0.009$, ΔRSNA: $P = 0.037$, Fig.7A&C). The pressor and sympathetic responses to passive muscle stretch were significantly suppressed by administration of HC067047 solution (ΔMAP: $P = 0.002$, ΔRSNA: $P = 0.019$, Bonferroni's multiple comparison test, Fig.7A&C). Main effects of trial and test solution as well as interaction were not observed in the measured ΔHR and ΔTension (Fig.7B&D).

Compared to saline administration, the control vehicle solution containing 0.07% DMSO and 0.03% ethanol did not affect the cardiovascular and sympathetic responses to passive stretch (saline (n = 4), before vs. after: ΔMAP: 19 ± 21 vs. 18 ± 17 mmHg; ΔHR: 3.2 ± 2.3 vs. 5.3 ± 6.3 beats/min ; ΔRSNA: 88 ± 59 vs. 91 ± 56%; ΔTension: 864 ± 145 vs. 862 ± 164 g; control vehicle solution (n = 4), before vs. after: ΔMAP: 22 ± 20 vs. 23 ± 24 mmHg; ΔHR: 4.5 ± 5.5 vs. 3.3 ± 3.7 beats/min ; ΔRSNA:89 ± 50 vs. 89 ± 52%; ΔTension: 841 ± 100 vs. 844 ± 143 g).

Discussion

The major findings from this investigation were 1) TRPV4 and peripherin were observed to be co-localized in DRG neurons innervating skeletal muscle, 2) the TRPV4 antagonist

HC067047 significantly lowered the sensitivity of small DRG neurons to mechanical stimulation, 3) HC067047 similarly decreased the response magnitude of group IV muscle afferents, and 4) HC067047 attenuated the pressor and sympathetic responses to passive stretch of hindlimb muscles in decerebrated rats.

Earlier studies have demonstrated that TRPV4 is highly expressed in DRG neurons of rats (Cao *et al.*, 2009; Cui *et al.*, 2020) and mice (Girard *et al.*, 2013). However, whether the DRG neurons expressing TRPV4 innervate skeletal muscle afferents has not been evaluated previously. In the present investigation, we observed 20.1 ± 10.1% of TRPV4-positive neurons in L4–6 DRGs innervating hindlimb muscle, and, among them 9.5 ± 6.1% of the neurons co-expressed the C-fibre marker, peripherin (Fig.1B&C). To the best of our knowledge, this is the first report showing that TRPV4 is expressed in DRGs innervating group IV muscle afferent C-fibres. It is well known that group IV muscle afferents contribute to the reflex cardiovascular increases evoked by exercise (Kaufman *et al.*, 1983; Hayes *et al.*, 2005). Our results, therefore, suggest that TRPV4 in skeletal muscle thin-fibre afferents are associated with the skeletal muscle reflex.

Mechanosensory transduction in DRG neurons is likely to be mediated by pressure directly activating mechanosensitive ion channels (Delmas *et al.*, 2011). However, little is known of the molecular mechanisms underlying this form of transduction (Gillespie & Walker, 2001). In the present study, the TRPV4 antagonist, HC067047, significantly suppressed MA currents in small DRG neurons (Fig.3A), while such a suppressive effect on mechanical threshold was not observed (by two-way ANOVA). However, even though 24% (5 out of 21) of DRG neurons increased mechanical threshold after application of the control solution, the application of HC067047 induced elevations in mechanical threshold in 71% of DRG neurons (15 out of 21). This rate seems to be consistent with previous findings demonstrating approximately 40–90% of DRG neurons express TRPV4 (Cao *et al.*, 2009; Girard *et al.*, 2013). In addition, HC067047 decreased the magnitude of MA currents and increased mechanical threshold in all types of MA currents (i.e. RA, IA, and SA). This suggests that TRPV4 does not account for the different types of MA current in DRG neurons. Taken together, our data suggest HC067047 suppresses the activity of TRPV4 expressed in DRG neurons.

We did not investigate DiI-labeled DRG neurons in whole-cell patch clamp experiments, therefore analysis of patch clamp measurements is not sufficient to identify the role of TRPV4 expressed in the mechanosensitive muscle afferent nerve terminals. That being said, small DRG neurons are known to subserve group IV afferent fibres (Harper & Lawson, 1985). Moreover, consistent with our whole-cell patch clamp results, HC067047 tended to increase mechanical threshold and significantly reduced the response magnitude of mechanically-evoked action potentials in EDL muscle group IV afferent fibres (Fig.5A&B). Given that HC067047 attenuated the response to mechanical stimulation in both DRG neurons and muscle group IV afferent fibres, the findings suggest that mechanical responsiveness of DRG neurons innervating skeletal muscle group IV fibres may be reduced by blocking TRPV4.

It is well known that group III fibres are predominately more mechanically-sensitive and group IV afferent fibres are generally more metabolically-sensitive (Kaufman *et al.*, 1983; Jankowski *et al.*, 2013; Teixeira & Vianna, 2022). That being said, in the current study we measured group IV instead of group III fibres to investigate the role of TRPV4 in mechanotransduction in rat skeletal muscle afferents. The rational for doing so was based in the fact that group IV fibres are polymodal in nature with many similarly responding to mechanical stimuli (Kumazawa & Mizumura, 1977). An earlier study demonstrated that almost 70% of group IV afferents are activated by local mechanical stimulation to the muscle (Bernardi & Neto, 1979). In addition, practically speaking, group IV fibres are more easily accessible and numerous compared to group III fibres (Taguchi *et al.*, 2005; Hotta *et al.*, 2015; Matsuda *et al.*, 2015; Hotta *et al.*, 2019b). For example, given a total of 1,480 afferents from a previous study, there were ~144 group Ia, 72 group Ib, 155 group II, 110 group III, and ~1,300 group IV units (Mitchell & Schmidt, 1983). These characteristics form the basis for assessing group IV muscle afferent responsiveness in the present study. Further investigations are warranted to clarify the role of TRPV4 as a mechanoreceptor in group III fibres.

The mechanically-sensitive channels or receptors that play a role in evoking muscle mechanoreflex activity remain largely undetermined. There are several reports which have primarily employed the use of mechano-sensitive channel inhibitors. For example, gadolinium, one of the more non-specific inhibitors of mechano-gated channels, attenuates the cardiovascular reflex response to both static contraction and tendon stretch in cats (Hayes & Kaufman, 2001). Moreover, the skeletal muscle exercise pressor reflex is attenuated by administration of the tarantula spider toxin Grammostola spatulata (GsMTx4, a mechano-gated cation Piezo channel inhibitor) in decerebrate rats (Copp *et al.*, 2016). To the best of our knowledge, this study is the first to demonstrate that blocking TRPV4 has inhibitory effects on the pressor and sympathetic responses to passive stretch. Therefore, our findings suggest that TRPV4 may be one of the mechanoreceptors responsible for activation of the muscle mechanoreflex.

Emerging evidence suggests that TRPV4 is a mechanosensitive channel that plays an important mechanotransduction role in endothelial cells (Swain & Liddle, 2021), chondrocytes (Du *et al.*, 2020) and smooth muscle cells (Chen *et al.*, 2022). The activation of TRPV4 is directly and indirectly mediated by mechanical force. The concept of direct activation suggests that the mechanical force acting on the cell membrane causes tension in the lipid bilayer, which induces changes in the structure and activity of mechanoreceptors (Kung, 2005; Pedersen & Nilius, 2007; Brohawn *et al.*, 2014). However, there is no evidence to support that TRPV4 acts as a mechanoreceptor with respect to mechanical force applied to the cell membrane (White *et al.*, 2016; Michalick & Kuebler, 2020). Therefore, TRPV4 may be activated by interacting with other cell compartments. In terms of an indirect activation pathway, TRPV4 activity is known to be stimulated by intracellular signaling including adenosine triphosphate (ATP) (Phelps *et al.*, 2010) and phospholipase A2 (PLA2) (Vriens *et al.*, 2005). An increase of interstitial ATP (Li *et al.*, 2005) and PLA2 activity (Vandenburgh *et al.*, 1993) is induced by muscle contraction and muscle stretch. Furthermore, recent studies in endothelial (Swain & Liddle, 2021) and pancreatic acinar cells (Swain *et al.*, 2020) have shown that TRPV4 channel opening is triggered by activation

of Piezo 1 which directly senses mechanical forces within the cell membrane (Coste *et al.*, 2010) and causes increased PLA2 activity (Swain *et al.*, 2020). Although such molecular candidates may indeed be associated with TRPV4 activation, further investigation is needed to evaluate the mechanisms underlying mechanotransduction via TRPV4 in DRG neurons and skeletal muscle afferents.

Surprisingly, in a corollary set of studies, we did not observe TRPV4 agonist-induced inward currents when exposing DRG neurons to the TRPV4 agonist, 4 α-phorbol 12,13-didecanoate (4-αPDD) (n = 29, the number of 4-αPDD-activated DRG neurons = 0) in additional whole-cell patch clamp experiments (data not shown). This finding is consistent with an earlier study showing that 4-αPDD-induced inward current was not observed in whole-cell patch clamp recordings from cultured rat bronchopulmonary sensory neurons (Gu *et al.*, 2016). On the other hand, Cao et al. reported that cultured embryonic rat DRG neurons responded to 4-αPDD in whole-cell patch clamp studies (Cao *et al.*, 2009). The reasons for the discrepancies between investigations are not readily clear. For example, in the current study, despite the fact that almost 90% of the adult rats investigated had DRG neurons expressing TRPV4, the number of 4-αPDD-positive DRG neurons was zero in stark contrast to the findings in embryonic DRG neurons (Cao *et al.*, 2009). Based on these results, it is likely that we could not detect 4-αPDD-evoked inward current in our study due to a decreased sensitivity of TRPV4 to 4-αPDD in the adult rat DRG neuron, perhaps due to differences in gene expression (Zhu & Oxford, 2011) or the composition of the cell membrane (Barabas *et al.*, 2014) as compared to embryonic DRG neurons. Consistent with our whole-cell patch clamp recording experiments, most of the muscle group IV afferent fibres (19 out of 21, 90.5%) did not respond to 4-αPDD nor were ABP and RSNA responses to muscle stretch affected by the agonist in decerebrate rats (0 out of 5, 100 %) (data not shown). These results are consistent with a recent study showing that intraarticular application of various kinds of TRPV4 agonists, including 4-αPDD, did not alter the neural discharge of C-fibres innervating the knee joints of rats (Richter *et al.*, 2019). Even though we could not detect the expression of TRPV4 by applying 4-αPDD, HC067047 attenuated the responses to mechanical stimulation of skeletal muscle, muscle group IV afferents and DRG neurons. It is plausible that HC067047 inhibited TRPV4 activity in DRG neurons and muscle group IV afferents, decreasing TRPV4 sensitivity to mechanical stimulation.

In conclusion, antagonism of TRPV4 by HC067047 attenuates mechanically activated currents in DRG neurons and response magnitude of afferent discharge to mechanical stimulation in thin-fibre muscle afferents. Further, HC067047 reduces the pressor and sympathetic responses to passive stretch of hindlimb muscles in decerebrated rats. These findings suggest that TRPV4, at least in part, plays a significant role in mechanotransduction and likely contributes to the expression of the skeletal muscle mechanoreflex during exercise.

Supplementary Material

Refer to Web version on PubMed Central for supplementary material.

ACKNOWLEDGEMENTS

We thank Martha Romero for her expert technical assistance.

GRANTS

This work was supported in part by National Heart, Lung, and Blood Institute (R01HL-151632) (to M.M.), Uehara Memorial Foundation (to A.F.), Grant-in-Aid for JSPS Research Fellows (21J20070) (to A.H.), and the JSPS Promotion of Joint International Research (Fostering Joint International Research (B) (22KK0154) (to N.H).

Biography

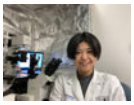

Ayumi Fukazawa received her MS and PhD from The University of Tokyo in Japan. She is currently a postdoctoral research fellow in the Department of Applied Clinical Research at the University of Texas Southwestern Medical Center. Her research focuses on investigating mechanisms underlying abnormal alterations in mechanotransduction in dorsal root ganglia neurons and somatosensory thin fibre afferents associated with the pathogenesis of disease (e.g. diabetes or Alzheimer's disease).

DATA AVAILABILITY STATEMENT

The data supporting the present findings are available from the corresponding author upon reasonable request.

Abbreviations:

DRG	dorsal root ganglion
TRPV4	transient receptor potential vanilloid 4
DiI	dioctadecyl-3,3,3,3-tetramethylindocarbocyanine perchlorate
EDL	extensor digitorum longus
ABP	arterial blood pressure
ECG	electrocardiograph
RSNA	renal sympathetic nerve activity
MAP	mean arterial pressure
HR	heart rate
RT	room temperature
MA	mechanically activated
RA	rapidly adapting

IA	inter-mediately adapting
SA	slowly adapting
DiI	1,1-dioctadecyl-3,3,3,3-tetramethylindocarbocyanine perchlorate
τ	time constant
ATP	adenosine triphosphate
PLA2	phospholipase A2
4-αPDD	4 α-phorbol 12,13-didecanoate
BW	body weight
PBS	phosphate-buffered saline
ANOVA	analysis of variance

Reference

Ariano MA, Armstrong RB & Edgerton VR. (1973). Hindlimb muscle fiber populations of five mammals. J Histochem Cytochem 21, 51–55. [PubMed: 4348494]

Barabas ME, Mattson EC, Aboualizadeh E, Hirschmugl CJ & Stucky CL. (2014). Chemical structure and morphology of dorsal root ganglion neurons from naive and inflamed mice. J Biol Chem 289, 34241–34249. [PubMed: 25271163]

Bernardi MM & Neto JP. (1979). Effects of abrupt and gradual withdrawal from long-term haloperidol treatment on open field behavior of rats. Psychopharmacology (Berl) 65, 247–250. [PubMed: 117495]

Brohawn SG, Su Z & MacKinnon R. (2014). Mechanosensitivity is mediated directly by the lipid membrane in TRAAK and TREK1 K+ channels. Proc Natl Acad Sci U S A 111, 3614–3619. [PubMed: 24550493]

Cao DS, Yu SQ & Premkumar LS. (2009). Modulation of transient receptor potential Vanilloid 4-mediated membrane currents and synaptic transmission by protein kinase C. Mol Pain 5, 5. [PubMed: 19208258]

Chen YL, Daneva Z, Kuppusamy M, Ottolini M, Baker TM, Klimentova E, Shah SA, Sokolowski JD, Park MS & Sonkusare SK. (2022). Novel Smooth Muscle Ca(2+)-Signaling Nanodomains in Blood Pressure Regulation. Circulation 146, 548–564. [PubMed: 35758040]

Christensen AP & Corey DP. (2007). TRP channels in mechanosensation: direct or indirect activation? Nat Rev Neurosci 8, 510–521. [PubMed: 17585304]

Copp SW, Kim JS, Ruiz-Velasco V & Kaufman MP. (2016). The mechano-gated channel inhibitor GsMTx4 reduces the exercise pressor reflex in decerebrate rats. J Physiol 594, 641–655. [PubMed: 26608396]

Coste B, Mathur J, Schmidt M, Earley TJ, Ranade S, Petrus MJ, Dubin AE & Patapoutian A. (2010). Piezo1 and Piezo2 are essential components of distinct mechanically activated cation channels. Science 330, 55–60. [PubMed: 20813920]

Cui YY, Li MY, Li YT, Ning JY, Gou XC, Shi J & Li YQ. (2020). Expression and functional characterization of transient receptor potential vanilloid 4 in the dorsal root ganglion and spinal cord of diabetic rats with mechanical allodynia. Brain Res Bull 162, 30–39. [PubMed: 32479780]

Delmas P, Hao J & Rodat-Despoix L. (2011). Molecular mechanisms of mechanotransduction in mammalian sensory neurons. Nat Rev Neurosci 12, 139–153. [PubMed: 21304548]

Drew LJ, Wood JN & Cesare P. (2002). Distinct mechanosensitive properties of capsaicin-sensitive and -insensitive sensory neurons. J Neurosci 22, Rc228. [PubMed: 12045233]

Du G, Li L, Zhang X, Liu J, Hao J, Zhu J, Wu H, Chen W & Zhang Q. (2020). Roles of TRPV4 and piezo channels in stretch-evoked Ca(2+) response in chondrocytes. Exp Biol Med (Maywood) 245, 180–189. [PubMed: 31791130]

Ducrocq GP, Estrada JA, Kim JS & Kaufman MP. (2019). Blocking the transient receptor potential vanilloid-1 does not reduce the exercise pressor reflex in healthy rats. Am J Physiol Regul Integr Comp Physiol 317, R576–r587. [PubMed: 31365302]

Filosa JA, Yao X & Rath G. (2013). TRPV4 and the regulation of vascular tone. J Cardiovasc Pharmacol 61, 113–119. [PubMed: 23107877]

Gillespie PG & Walker RG. (2001). Molecular basis of mechanosensory transduction. Nature 413, 194–202. [PubMed: 11557988]

Girard BM, Merrill L, Malley S & Vizzard MA. (2013). Increased TRPV4 expression in urinary bladder and lumbosacral dorsal root ganglia in mice with chronic overexpression of NGF in urothelium. J Mol Neurosci 51, 602–614. [PubMed: 23690258]

Grant AD, Cottrell GS, Amadesi S, Trevisani M, Nicoletti P, Materazzi S, Altier C, Cenac N, Zamponi GW, Bautista-Cruz F, Lopez CB, Joseph EK, Levine JD, Liedtke W, Vanner S, Vergnolle N, Geppetti P & Bunnett NW. (2007). Protease-activated receptor 2 sensitizes the transient receptor potential vanilloid 4 ion channel to cause mechanical hyperalgesia in mice. J Physiol 578, 715–733. [PubMed: 17124270]

Grundy D (2015). Principles and standards for reporting animal experiments in The Journal of Physiology and Experimental Physiology. J Physiol 593, 2547–2549. [PubMed: 26095019]

Gu QD, Moss CR, 2nd, Kettelhut KL, Gilbert CA & Hu H (2016). Activation of TRPV4 Regulates Respiration through Indirect Activation of Bronchopulmonary Sensory Neurons. Front Physiol 7, 65. [PubMed: 26973533]

Harper AA & Lawson SN. (1985). Conduction velocity is related to morphological cell type in rat dorsal root ganglion neurones. J Physiol 359, 31–46. [PubMed: 3999040]

Harraz OF, Longden TA, Hill-Eubanks D & Nelson MT. (2018). PIP(2) depletion promotes TRPV4 channel activity in mouse brain capillary endothelial cells. Elife 7.

Hayes SG & Kaufman MP. (2001). Gadolinium attenuates exercise pressor reflex in cats. Am J Physiol Heart Circ Physiol 280, H2153–2161. [PubMed: 11299217]

Hayes SG, Kindig AE & Kaufman MP. (2005). Comparison between the effect of static contraction and tendon stretch on the discharge of group III and IV muscle afferents. J Appl Physiol (1985) 99, 1891–1896. [PubMed: 15994238]

Hori A, Hotta N, Fukazawa A, Estrada JA, Katanosaka K, Mizumura K, Sato J, Ishizawa R, Kim HK, Iwamoto GA, Vongpatanasin W, Mitchell JH, Smith SA & Mizuno M. (2022). Insulin potentiates the response to capsaicin in dorsal root ganglion neurons in vitro and muscle afferents ex vivo in normal healthy rodents. J Physiol 600, 531–545. [PubMed: 34967443]

Hotta N, Katanosaka K, Mizumura K, Iwamoto GA, Ishizawa R, Kim HK, Vongpatanasin W, Mitchell JH, Smith SA & Mizuno M. (2019a). Insulin potentiates the response to mechanical stimuli in small dorsal root ganglion neurons and thin fibre muscle afferents in vitro. J Physiol 597, 5049–5062. [PubMed: 31468522]

Hotta N, Kubo A & Mizumura K. (2015). Effect of protons on the mechanical response of rat muscle nociceptive fibers and neurons in vitro. Neurosci Res 92, 46–52. [PubMed: 25452124]

Hotta N, Kubo A & Mizumura K. (2019b). Chondroitin sulfate attenuates acid-induced augmentation of the mechanical response in rat thin-fiber muscle afferents in vitro. J Appl Physiol (1985) 126, 1160–1170. [PubMed: 30763166]

Hu J & Lewin GR. (2006). Mechanosensitive currents in the neurites of cultured mouse sensory neurones. J Physiol 577, 815–828. [PubMed: 17038434]

Jankowski MP, Rau KK, Ekmann KM, Anderson CE & Koerber HR. (2013). Comprehensive phenotyping of group III and IV muscle afferents in mouse. J Neurophysiol 109, 2374–2381. [PubMed: 23427306]

Kaufman MP, Longhurst JC, Rybicki KJ, Wallach JH & Mitchell JH. (1983). Effects of static muscular contraction on impulse activity of groups III and IV afferents in cats. J Appl Physiol Respir Environ Exerc Physiol 55, 105–112. [PubMed: 6309712]

Kaufman MP, Waldrop TG, Rybicki KJ, Ordway GA & Mitchell JH. (1984). Effects of static and rhythmic twitch contractions on the discharge of group III and IV muscle afferents. Cardiovasc Res 18, 663–668. [PubMed: 6498873]

Kubo A, Katanosaka K & Mizumura K. (2012). Extracellular matrix proteoglycan plays a pivotal role in sensitization by low pH of mechanosensitive currents in nociceptive sensory neurones. J Physiol 590, 2995–3007. [PubMed: 22570376]

Kumazawa T & Mizumura K. (1977). Thin-fibre receptors responding to mechanical, chemical, and thermal stimulation in the skeletal muscle of the dog. J Physiol 273, 179–194. [PubMed: 599419]

Kung C (2005). A possible unifying principle for mechanosensation. Nature 436, 647–654. [PubMed: 16079835]

Lawson SN & Waddell PJ. (1991). Soma neurofilament immunoreactivity is related to cell size and fibre conduction velocity in rat primary sensory neurons. J Physiol 435, 41–63. [PubMed: 1770443]

Li J, King NC & Sinoway LI. (2005). Interstitial ATP and norepinephrine concentrations in active muscle. Circulation 111, 2748–2751. [PubMed: 15911708]

Liedtke W, Choe Y, Martí-Renom MA, Bell AM, Denis CS, Sali A, Hudspeth AJ, Friedman JM & Heller S. (2000). Vanilloid receptor-related osmotically activated channel (VR-OAC), a candidate vertebrate osmoreceptor. Cell 103, 525–535. [PubMed: 11081638]

Loukin S, Zhou X, Su Z, Saimi Y & Kung C. (2010). Wild-type and brachyolmia-causing mutant TRPV4 channels respond directly to stretch force. J Biol Chem 285, 27176–27181. [PubMed: 20605796]

Matsuda T, Kubo A, Taguchi T & Mizumura K. (2015). ATP decreases mechanical sensitivity of muscle thin-fiber afferents in rats. Neurosci Res 97, 36–44. [PubMed: 25862944]

Michalick L & Kuebler WM. (2020). TRPV4-A Missing Link Between Mechanosensation and Immunity. Front Immunol 11, 413. [PubMed: 32210976]

Mitchell JH, Schmidt RF. (1983). Handbook of Physiology, Cardiovascular reflex control by afferent fibers from skeletal muscle receptors. pp. 623–658. Oxford University Press, Oxford.

Mizuno M, Mitchell JH, Crawford S, Huang CL, Maalouf N, Hu MC, Moe OW, Smith SA & Vongpatanasin W. (2016). High dietary phosphate intake induces hypertension and augments exercise pressor reflex function in rats. Am J Physiol Regul Integr Comp Physiol 311, R39–48. [PubMed: 27170660]

Pedersen SF & Nilius B. (2007). Transient receptor potential channels in mechanosensing and cell volume regulation. Methods Enzymol 428, 183–207. [PubMed: 17875418]

Phelps CB, Wang RR, Choo SS & Gaudet R. (2010). Differential regulation of TRPV1, TRPV3, and TRPV4 sensitivity through a conserved binding site on the ankyrin repeat domain. J Biol Chem 285, 731–740. [PubMed: 19864432]

Richter F, Segond von Banchet G & Schaible HG. (2019). Transient Receptor Potential vanilloid 4 ion channel in C-fibres is involved in mechanonociception of the normal and inflamed joint. Sci Rep 9, 10928. [PubMed: 31358810]

Schiller AM, Hong J, Xia Z & Wang HJ. (2019). Increased Brain-Derived Neurotrophic Factor in Lumbar Dorsal Root Ganglia Contributes to the Enhanced Exercise Pressor Reflex in Heart Failure. Int J Mol Sci 20.

Silverman J, Garnett NL, Giszter SF, Heckman CJ, 2nd, Kulpa-Eddy JA, Lemay MA, Perry CK & Pinter M (2005). Decerebrate mammalian preparations: unalleviated or fully alleviated pain? A review and opinion. Contemp Top Lab Anim Sci 44, 34–36. [PubMed: 16050666]

Smith SA, Downey RM, Williamson JW & Mizuno M. (2014). Autonomic dysfunction in muscular dystrophy: a theoretical framework for muscle reflex involvement. Front Physiol 5, 47. [PubMed: 24600397]

Stebbins CL, Brown B, Levin D & Longhurst JC. (1988). Reflex effect of skeletal muscle mechanoreceptor stimulation on the cardiovascular system. J Appl Physiol (1985) 65, 1539–1547. [PubMed: 3182517]

Strotmann R, Harteneck C, Nunnenmacher K, Schultz G & Plant TD. (2000). OTRPC4, a nonselective cation channel that confers sensitivity to extracellular osmolarity. Nat Cell Biol 2, 695–702. [PubMed: 11025659]

Swain SM & Liddle RA. (2021). Piezo1 acts upstream of TRPV4 to induce pathological changes in endothelial cells due to shear stress. J Biol Chem 296, 100171. [PubMed: 33298523]

Swain SM, Romac JM, Shahid RA, Pandol SJ, Liedtke W, Vigna SR & Liddle RA. (2020). TRPV4 channel opening mediates pressure-induced pancreatitis initiated by Piezo1 activation. J Clin Invest 130, 2527–2541. [PubMed: 31999644]

Taguchi T, Sato J & Mizumura K. (2005). Augmented mechanical response of muscle thin-fiber sensory receptors recorded from rat muscle-nerve preparations in vitro after eccentric contraction. J Neurophysiol 94, 2822–2831. [PubMed: 16160095]

Teixeira AL & Vianna LC. (2022). The exercise pressor reflex: An update. Clin Auton Res 32, 271–290. [PubMed: 35727398]

Vandenburgh HH, Shansky J, Karlisch P & Solerssi RL. (1993). Mechanical stimulation of skeletal muscle generates lipid-related second messengers by phospholipase activation. J Cell Physiol 155, 63–71. [PubMed: 8468370]

Victor RG, Rotto DM, Pryor SL & Kaufman MP. (1989). Stimulation of renal sympathetic activity by static contraction: evidence for mechanoreceptor-induced reflexes from skeletal muscle. Circ Res 64, 592–599. [PubMed: 2917383]

Vriens J, Owsianik G, Fisslthaler B, Suzuki M, Janssens A, Voets T, Morisseau C, Hammock BD, Fleming I, Busse R & Nilius B. (2005). Modulation of the Ca2 permeable cation channel TRPV4 by cytochrome P450 epoxygenases in vascular endothelium. Circ Res 97, 908–915. [PubMed: 16179585]

Wakatsuki K YTU, Matsubara T, Nasu T, Mizumura K & Taguchi T. (2021). Peripheral nociceptive mechanisms in an experimental rat model of fibromyalgia induced by repeated cold stress. Neurosci Res 162, 22–30. [PubMed: 31891739]

Watanabe H, Davis JB, Smart D, Jerman JC, Smith GD, Hayes P, Vriens J, Cairns W, Wissenbach U, Prenen J, Flockerzi V, Droogmans G, Benham CD & Nilius B. (2002a). Activation of TRPV4 channels (hVRL-2/mTRP12) by phorbol derivatives. J Biol Chem 277, 13569–13577. [PubMed: 11827975]

Watanabe H, Vriens J, Suh SH, Benham CD, Droogmans G & Nilius B. (2002b). Heat-evoked activation of TRPV4 channels in a HEK293 cell expression system and in native mouse aorta endothelial cells. J Biol Chem 277, 47044–47051. [PubMed: 12354759]

White JP, Cibelli M, Urban L, Nilius B, McGeown JG & Nagy I. (2016). TRPV4: Molecular Conductor of a Diverse Orchestra. Physiol Rev 96, 911–973. [PubMed: 27252279]

Williamson JW, Mitchell JH, Olesen HL, Raven PB & Secher NH. (1994). Reflex increase in blood pressure induced by leg compression in man. J Physiol 475, 351–357. [PubMed: 8021841]

Xing J & Li J. (2017). TRPA1 Function in Skeletal Muscle Sensory Neurons Following Femoral Artery Occlusion. Cell Physiol Biochem 42, 2307–2317. [PubMed: 28848196]

Xing J, Lu J & Li J. (2015). ASIC3 contributes to the blunted muscle metaboreflex in heart failure. Med Sci Sports Exerc 47, 257–263. [PubMed: 24983337]

Zhang Y, Qin W, Qian Z, Liu X, Wang H, Gong S, Sun YG, Snutch TP, Jiang X & Tao J. (2014). Peripheral pain is enhanced by insulin-like growth factor 1 through a G protein-mediated stimulation of T-type calcium channels. Sci Signal 7, ra94. [PubMed: 25292213]

Zhang Y, Wang YH, Ge HY, Arendt-Nielsen L, Wang R & Yue SW. (2008). A transient receptor potential vanilloid 4 contributes to mechanical allodynia following chronic compression of dorsal root ganglion in rats. Neurosci Lett 432, 222–227. [PubMed: 18206306]

Zhu W & Oxford GS. (2011). Differential gene expression of neonatal and adult DRG neurons correlates with the differential sensitization of TRPV1 responses to nerve growth factor. Neurosci Lett 500, 192–196. [PubMed: 21741445]

KEYPOINT

- Although a mechanical stimulus to skeletal muscle reflexively activates the sympathetic nervous system, the receptors responsible for mechanotransduction in skeletal muscle thin fibre afferents have not been fully identified.
- Evidence suggests that TRPV4 is mechanosensitive channel that plays an important role in mechanotransduction within various organs.
- Immunocytochemical staining demonstrates that TRPV4 is expressed in group IV skeletal muscle afferents. In addition, we show that the TRPV4 antagonist, HC067047, decreases the responsiveness of thin fibre afferents to mechanical stimulation at the muscle tissue level as well as at the level of dorsal root ganglion neurons. Moreover, we demonstrate that intraarterial HC067047 injection attenuates the sympathetic and pressor responses to passive muscle stretch in decerebrate rats.
- These data suggests that antagonism of TRPV4 attenuates mechanotransduction in skeletal muscle afferents.
- The present study demonstrates a probable physiological role for TRPV4 in the regulation of mechanical sensation in somatosensory thin fibre muscle afferents.

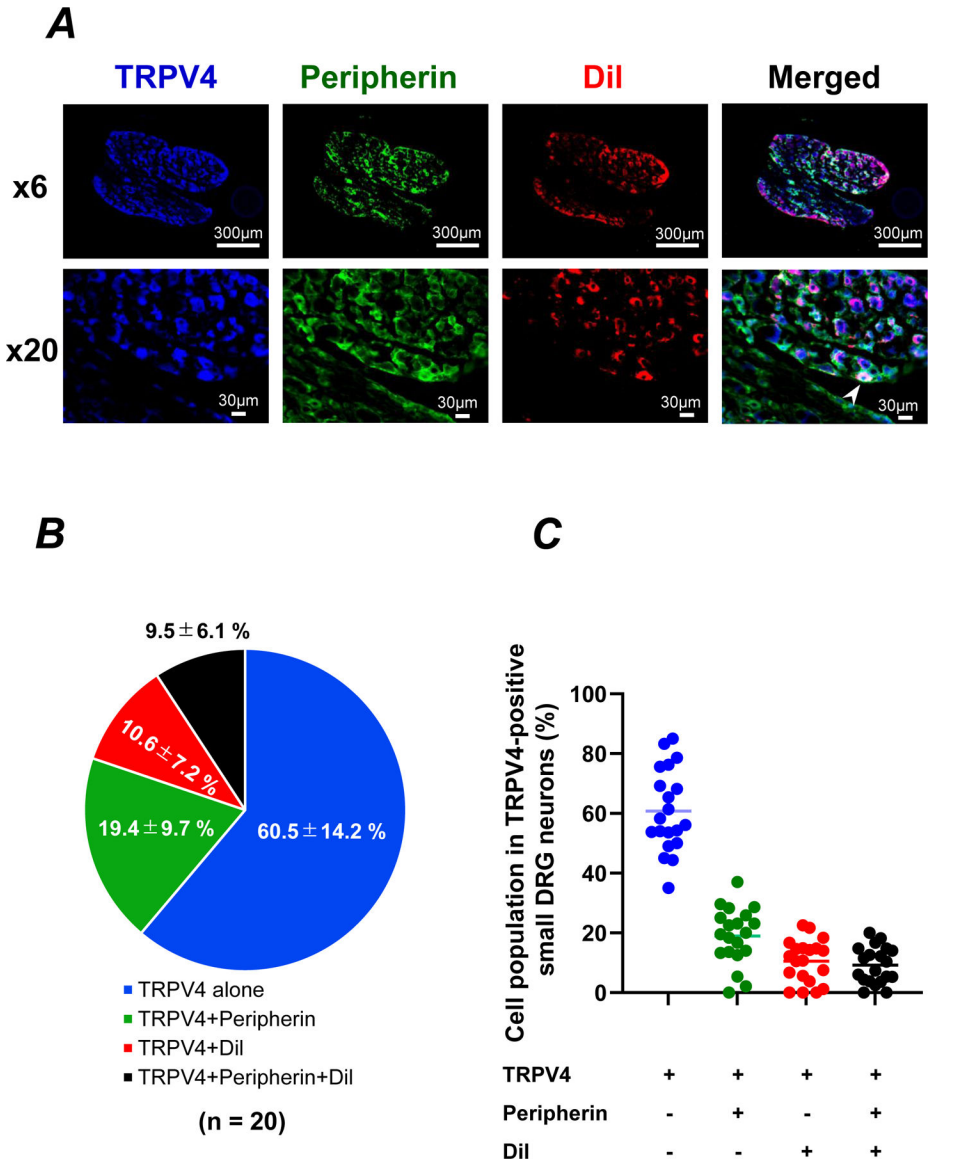

Figure 1. Co-localization of transient receptor potential vanilloid 4 (TRPV4) and peripherin in L4-L6 dorsal root ganglion (DRG) neurons subserving skeletal muscle sensory neurons in rats

A, representative images showing the expression of TRPV4, and peripherin-positive neurons in DiI retrograde-labeled L4-L6 DRGs innervating gastrocnemius muscle. Merged immunofluorescence images show co-localization of TRPV4 and peripherin in DiI-labeled DRG neurons (white arrowhead). Magnifications: ×6 and ×20. Scale bars: 300 or 30 μm. *B*, the percentages of peripherin- and/or DiI-positive neurons in TRPV4-positive small DRG neurons. Data are shown as the mean. ± SD. *C*, individual data obtained from distinct sections. A total of 20 DRG sections were collected from three rats.

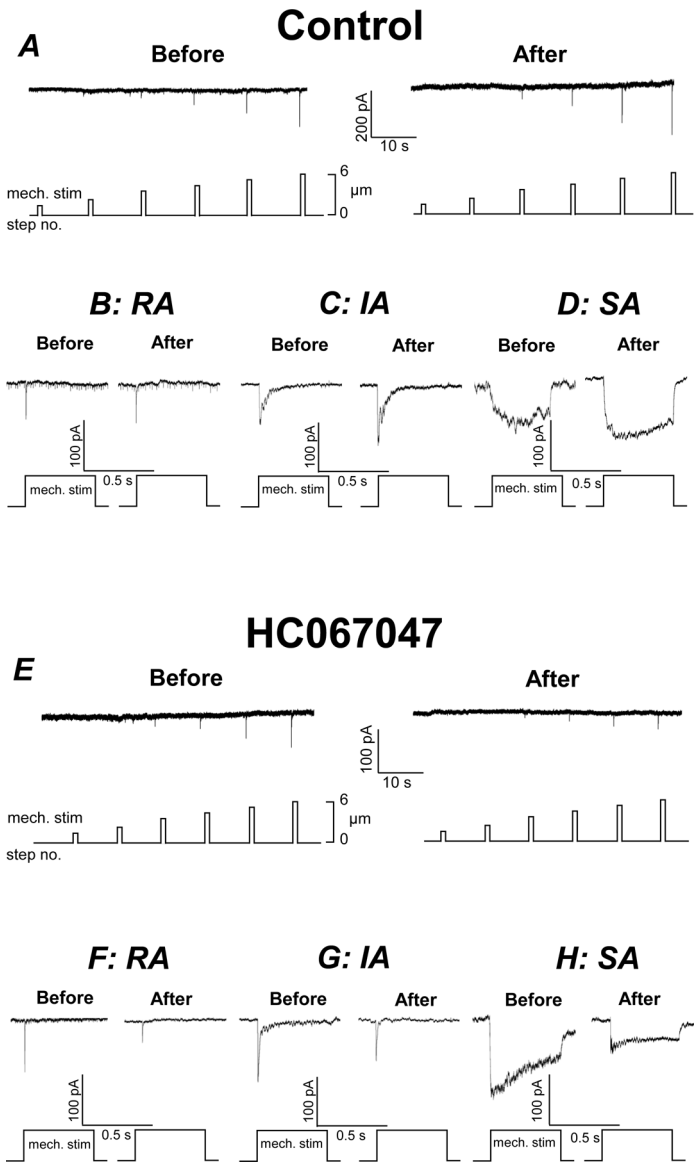

Figure 2. Sample recordings of mechanically-activated (MA) inward currents before and after application of HEPES-buffered solution (Control) or TRPV4 antagonist solution (HC067047)

A, continuous sample recordings of MA current before and 5 min after the application of HEPES buffered solution (control solution). From top to bottom: raw current recordings in voltage clamp mode, representations of mechanical stimuli (see details in Methods) and step numbers of mechanical stimuli. *B*, *C* and *D*, samples of MA currents (rapidly adapting (RA); inter-mediately adapting (IA); and slowly adapting (SA)) at the same intensities that mechanical threshold was marked before the application of control solution, respectively. These currents were recorded from the different cells. *E*, continuous sample recording of MA current before and 5 min after the application of 1 µM HC067047 solution (TRPV4 antagonist solution). *F*, *G*, and *H*, samples of MA currents (RA, IA, SA) at the same intensities that mechanical threshold was marked before the application of HC067047 solution, respectively. These currents were recorded from the different cells.

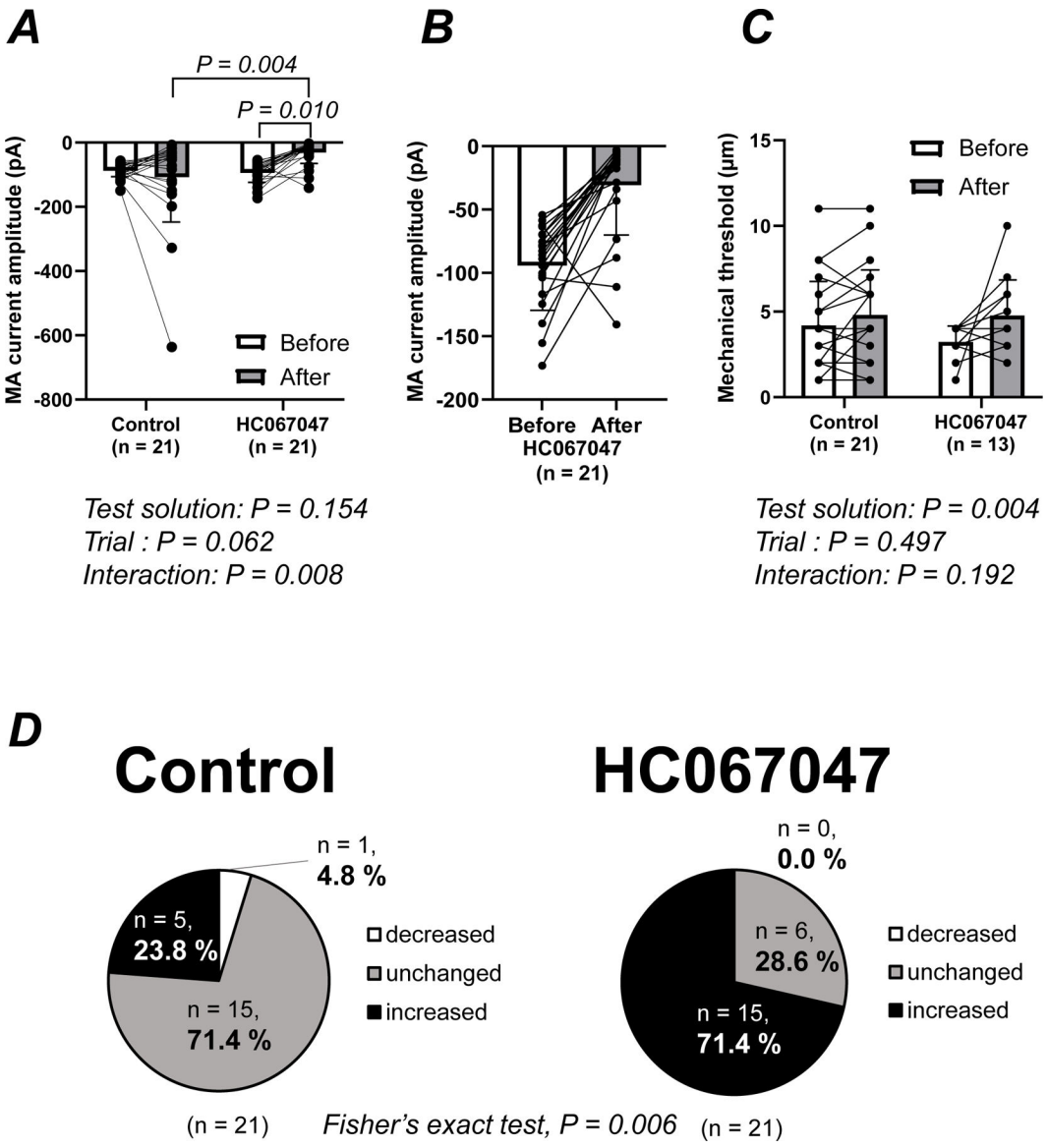

Figure 3. Average changes in MA current amplitude (A and B), average changes in mechanical threshold (C) and population changes in mechanical threshold (D) in small DRG neurons from before to 5 min after application of HEPES-buffered solution (control) or TRPV4 antagonist solution (HC067047)

B, enlarged view of MA current amplitude of HC067047 trials in *A*. *D*, DRG neurons were classified by the difference in mechanical threshold (ΔMt) from the value before test solutions were applied compared to after the test applications were applied: *decreased*, ΔM ≤−2 steps; *unchanged*, ΔMt ≤ ±1 step; and *increased*, ΔMt ≥ 2 steps. Data are shown as the mean. ± SD. Two-way ANOVA was performed, followed by the Bonferroni's multiple comparison test (*A* and *C*). Fischer's exact test was performed (*D*). DRGs were collected from 10 rats and 42 small DRG neurons were assessed.

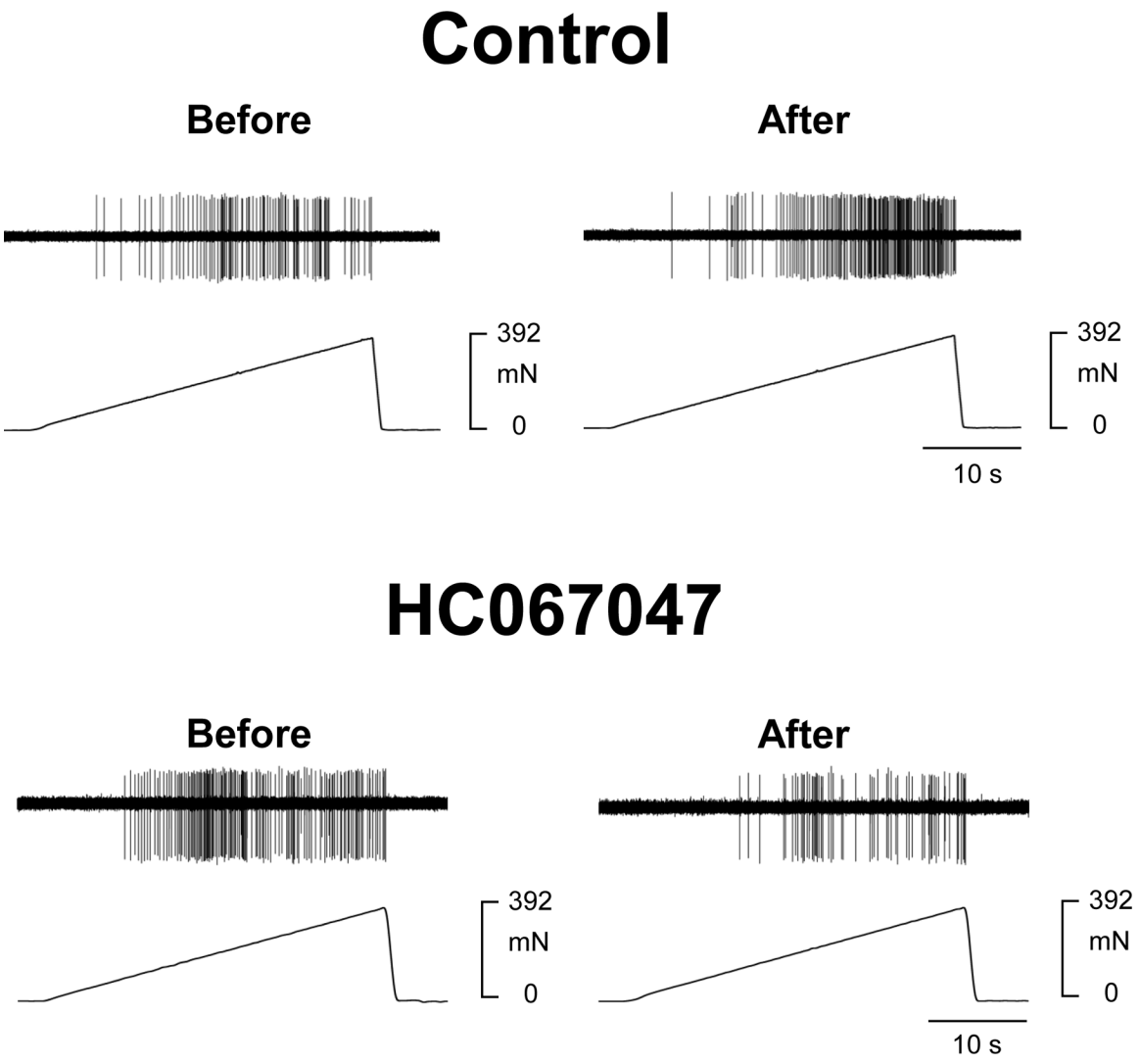

Figure 4. Response of group IV muscle afferents to mechanical stimulation before and 10 min after intramuscular injection of Krebs buffer solution (control) or TRPV4 antagonist solution (HC067047)

From top to bottom; the raw recording of individual group IV fibre activity and intensity of mechanical stimuli.

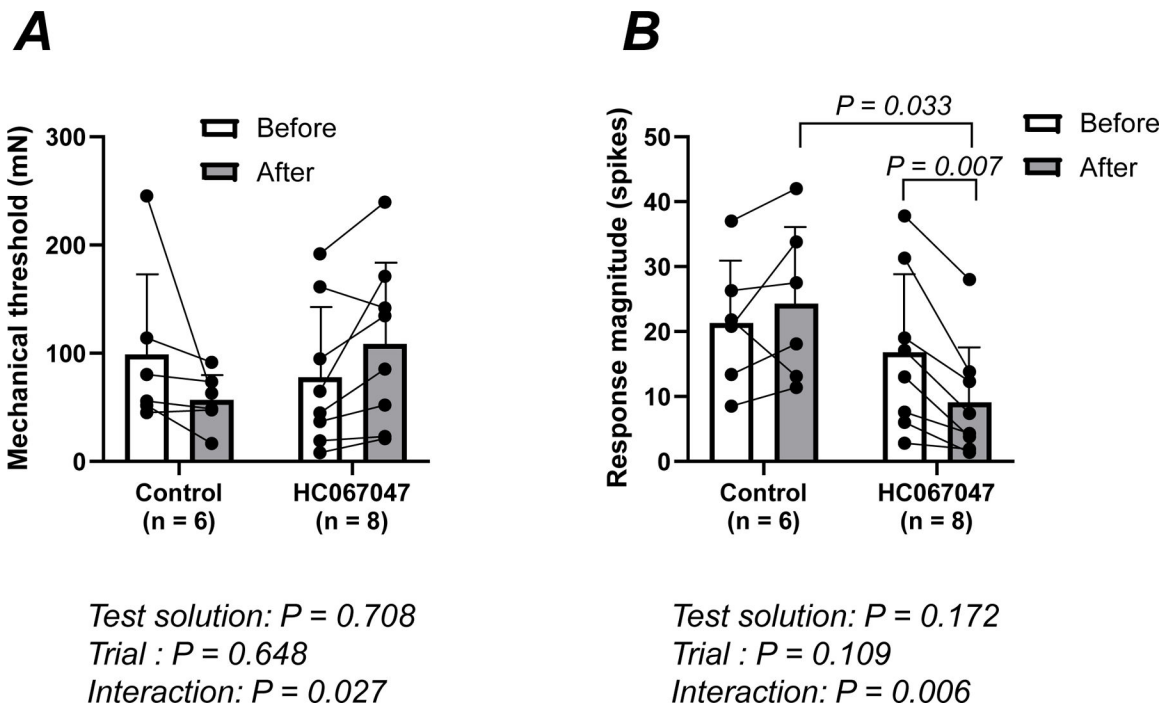

Figure 5. Average changes in mechanical threshold (A) and response of magnitude (B) in group IV muscle afferents from before to 10 min after intramuscular injection of Krebs buffer solution (control) or TRPV4 antagonist solution (HC067047)

Data are shown as the mean ± SD. Two-way ANOVA was performed, followed by the Bonferroni's multiple comparison test. EDL muscle with the common peroneal nerve was isolated from 12 rats and 14 mechanosensitive group IV fibres were assessed.

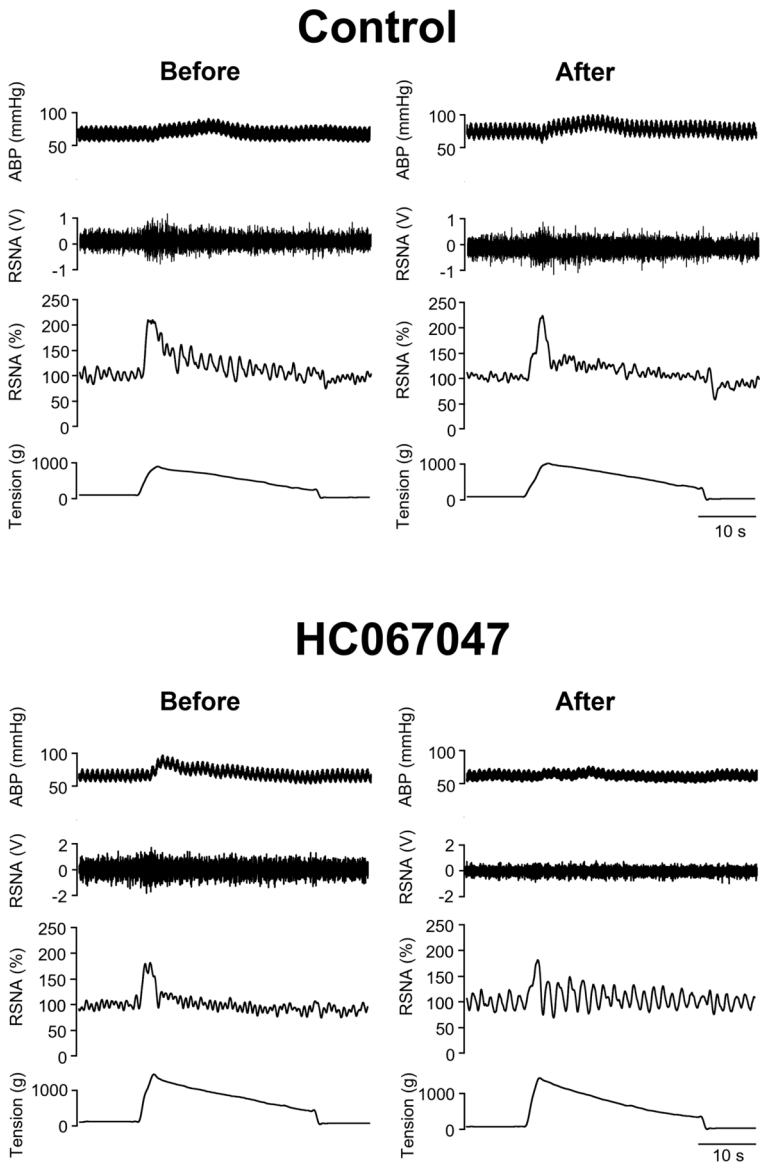

Figure 6. Arterial blood pressure (ABP) and sympathetic responses to activation of the muscle mechanoreflex via passive stretch before and 5 min after intraarterial injection of saline (control) or TRPV4 antagonist solution (HC067047)

From top to bottom; the raw recording of ABP, raw and normalized renal sympathetic nerve activity (RSNA), and tension.

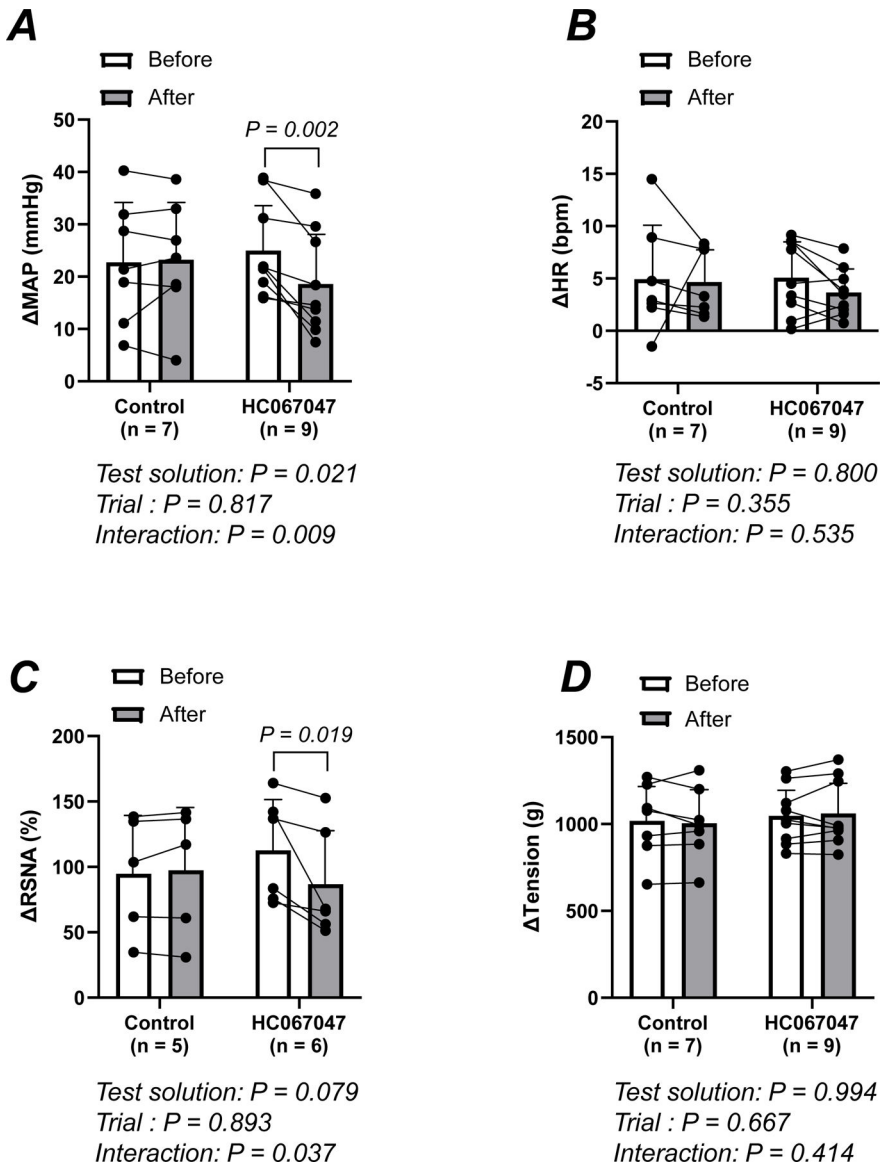

Figure 7. Peak changes in mean arterial pressure (MAP) (A), heart rate (HR) (B), renal sympathetic nerve activity (RSNA) (C), and developed tension (D) during passive hindlimb muscle stretch before to 5 min after intraarterial injection of saline (control) or TRPV4 antagonist solution (HC067047)

Data are shown as the mean ± SD. Two-way ANOVA was performed, followed by the Bonferroni's multiple comparison test. ABP in 16, HR in 16, RSNA in 11 and tension in 16 rats were assessed.